



**HAL**  
open science

## Effect of film thickness on the dielectric properties and charge storage in PMMA thin films

J. Orrit-Prat, Laurent Boudou, Christina Villeneuve-Faure, Gilbert Teyssedre, Behar S., Ressier L., Diaz R.

### ► To cite this version:

J. Orrit-Prat, Laurent Boudou, Christina Villeneuve-Faure, Gilbert Teyssedre, Behar S., et al.. Effect of film thickness on the dielectric properties and charge storage in PMMA thin films. ICSD : IEEE International Conference on Solid Dielectrics Bologna, Italy, Jun 2013, Bologna, Italy. pp.350-353, <10.1109/ICSD.2013.6619883>. <hal-03942789>

**HAL Id: hal-03942789**

**<https://hal.science/hal-03942789v1>**

Submitted on 18 Jan 2023

HAL is a multi-disciplinary open access archive for the deposit and dissemination of scientific research documents, whether they are published or not. The documents may come from teaching and research institutions in France or abroad, or from public or private research centers.

L'archive ouverte pluridisciplinaire HAL, est destinée au dépôt et à la diffusion de documents scientifiques de niveau recherche, publiés ou non, émanant des établissements d'enseignement et de recherche français ou étrangers, des laboratoires publics ou privés.



HAL Authorization

# Effect of film thickness on the dielectric properties and charge storage in PMMA thin films

Jordi Orrit-Prat, Laurent Boudou, Christina Villeneuve, Gilbert Teysseire

Université de Toulouse & CNRS, LAPLACE, Université P. Sabatier, Bat 3R3, 118 route de Narbonne, 31062 Toulouse, France  
jordi.orr@laplace.univ-tlse.fr

Samuel Behar, Laurence Ressler, Régis Diaz  
Université de Toulouse, LPCNO, INSA-UPS-CNRS,  
135 avenue de Rangueil, F-31077  
Toulouse, France

**Abstract**—In this work, we demonstrate the excellent charge retention capability of spin-coated Polymethylmethacrylate (PMMA) 200 nm thin films previously charged by atomic force microscopy. In order to elucidate the mechanisms involved in the charge transport and charge storage in PMMA films, the conductivity of 200nm thin PMMA films was analyzed on Metal-Insulation-Metal (MIM) structures. A wide range of electric fields was applied on these structures and the charge and discharge currents were recorded. The thermal dependence of the conduction mechanisms was determined for temperatures below the PMMA glass transition temperature. These results were compared to those obtained for 50 $\mu$ m thick PMMA films in which the conductivity appears much smaller. The effects of PMMA thickness on charge transport are discussed.

**Keywords**—Polymethylmethacrylate; thin films; charge writing by atomic force microscopy; Kelvin force microscopy; conductivity

## I. INTRODUCTION

Polymethylmethacrylate (PMMA) is a polymeric material widely used in electrical and optical applications. Recently, it has been introduced in the Organic Thin Film Transistors (OTFT) [1], showing excellent properties as gate dielectric or buffer layer. This has motivated some research on the electrical properties of PMMA thin films [2]. In parallel, other innovative fields incorporate the use of PMMA thin films. It is the case of nanoxerography [3], which consists in the directed assembly of colloidal nano-objects onto electrostatically patterned dielectric surfaces. This technique can lead to the fabrication of nanodevices in various domains such as electronics, optics or sensor applications [4]. In fact, PMMA thin films can be efficiently electrostatically patterned by different charging methods, like Atomic Force Microscopy (AFM) charge writing [3], electrical microcontact printing [5] or electrical nanoimprint [6].

Nonetheless, some well-known characteristics of PMMA are no longer valid for nanometric-thick films. Film thickness strongly affects the molecular dynamics and the glass transition temperature ( $T_g$ ) [7]. With regard to the specific dielectric characteristics, the breakdown strength depends on the physical dimensions [2]. Charge transport mechanisms and charge retention capability would also be influenced by the

film thickness, which can be an important issue for nanoxerography applications. Better understanding of the electrical conduction in PMMA thin films would give more information about the breakdown mechanism and polymer characteristics at the nanometric scale, which are related to several promising applications.

In this study, after charge writing into PMMA films of two different thicknesses (200nm and 50 $\mu$ m) by AFM, charge retention was followed by Kelvin force microscopy (KFM). Conduction characteristics of these PMMA films were also analyzed from I(V) measurements. Finally, the thickness impact on dielectric properties, charge transport and charge storage of PMMA is discussed.

## II. EXPERIMENTAL

### A. Material and samples

50 $\mu$ m thick commercial films were obtained from Goodfellow (GF). Two kinds of 200nm thin PMMA films were elaborated by spin coating on n-doped ( $10^{15}$  cm $^{-3}$ ) silicon substrates and glass substrates. The first ones (named SA thin films) were elaborated from PMMA powder provided by Sigma Aldrich (SA) dissolved into methyl isobutyl ketone (MIBK). The second ones (named GF thin films) were prepared from above-mentioned 50 $\mu$ m thick commercial films.

### B. AFM charge writing and surface potential measurements by KFM

AFM charge writing was performed on 200nm SA and GF thin PMMA films spin coated on silicon substrates and on 50 $\mu$ m thick PMMA films. 20  $\mu$ m x10  $\mu$ m positively (resp. negatively) charged rectangles were written into each PMMA film by applying voltage pulses to a conductive AFM tip with an external generator. The z-feedback was adjusted to control the tip-film separation during charge writing. The pulse length and frequency were fixed at 1 ms and 50 Hz, respectively, while the tip velocity was fixed at 10 $\mu$ m/s.

After AFM charge writing, amplitude modulation KFM was used to measure the surface potentials of charged patterns (lift height = 50nm). Charge retention in PMMA films was measured by recording successively 12 KFM images.

### C. Electrical conduction characteristics in PMMA films

For 50 $\mu\text{m}$  thick films, 30nm thick silver electrodes with a diameter of 5 $\mu\text{m}$  were deposited by sputtering on each face. For both SA and GF thin films, two 150nm thick parallel silver stripes were deposited on glass substrates before spin coating 200nm thin PMMA films. Two columns of five silver stripes perpendicular to the previous ones were finally deposited on top of the PMMA films. Thus, 10 Metal-Insulator-Metal (MIM) regions of 12 mm<sup>2</sup> were available on each sample.

The conduction measurements on PMMA films were performed in a chamber with a temperature-controlled helium environment. The samples were polarized at constant temperatures for 1000 seconds and then short-circuited for the same duration. The polarization and depolarization currents were recorded by a Keithley 6512 electrometer. Several electric fields conditions were applied for each temperature.

## III. RESULTS

### A. KFM measurements

Fig. 1 shows a typical KFM image just after charge writing in a 200nm SA thin film spin-coated on a silicon substrate. The upper negatively charged rectangle written with -75V voltage pulses present a surface potential of -10.0V whereas the lower positively charged rectangle written with +75V voltage pulses has a surface potential of +9.6V. Charge writing on 200nm GF thin films gave similar results. The same experiments performed for 50 $\mu\text{m}$  thick films revealed that charge injection is far less efficient than charge injection in 200nm thin films. A stronger dissymmetry of charge injection between negative and positive charges was also observed: the rectangle written with -75V (resp. +75V) voltage pulses presented a surface potential of -6.5 V (resp. +4.8V).

The temporal evolution of the surface potential of the negatively and positively charged rectangles written in 200nm SA thin films and 50 $\mu\text{m}$  thick films are plotted in Fig. 2. Measurements on 200nm GF thin films (data not shown) revealed no significant difference with those obtained on 200nm SA thin films. Fig. 2 reveals a strong decrease of the surface potential of charged rectangles during the 30 first minutes after charge writing for thin and thick films. The charge loss is weaker after, especially for positive charges into 200 nm SA thin films (less than 25% of charge loss during the

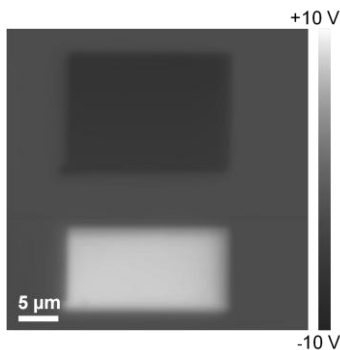


Fig. 1 KFM image of negatively and positively charged rectangles taken just after AFM charge writing in a 200nm SA PMMA thin film

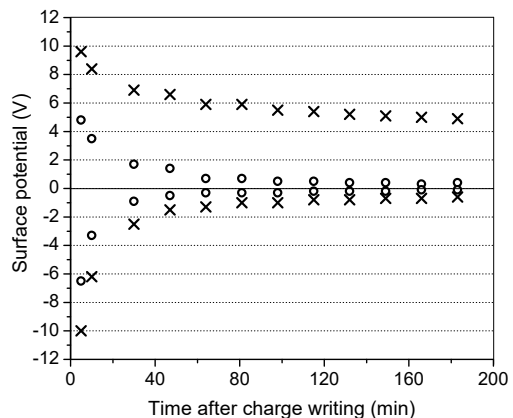


Fig. 2 Temporal evolution of the surface potential of negatively and positively charged rectangles written by AFM in 200nm SA thin films (x) and 50 $\mu\text{m}$  thick films (o)

following 2 hours). The charge retention of thin films appears to be much better than that of thick films, especially for positive charges. About 50% of the positive charges written in 200nm PMMA thin films are still present after 3 hours, making PMMA an excellent electret.

### B. Conductivity measurements

#### 1) 200nm thin films

Charge and discharge currents were measured at different temperatures (25-90 $^{\circ}\text{C}$ ) below  $T_g$  (around 100 $^{\circ}\text{C}$ ) and for several fields conditions (in the 0.5-250kV/mm range). Fig. 3 presents a plot of the conduction current density as a function of the applied electric field, for various temperatures in the above-mentioned ranges, in case of the 200nm GF thin films. A linear dependence between the conduction current density and the applied electric field is observed in all cases. This implies that the dominant charge transport mechanism is the ohmic conduction, related to the following expression:

$$J = \sigma F \quad (1)$$

where  $J$  is the current density,  $\sigma$  the conductivity and  $F$  the applied electric field. The  $\sigma$  values obtained from the linear fits made on the experimental data range from  $4.13 \times 10^{-15} \text{S/m}$  at 25 $^{\circ}\text{C}$  up to  $1.09 \times 10^{-12} \text{S/m}$  at 90 $^{\circ}\text{C}$ .

On the other hand, the conductivity dependence on the temperature, presented in Fig. 4 for the same PMMA films, can be addressed by the Arrhenius law, given below:

$$\sigma = \sigma_0 e^{-\frac{E_a}{kT}} \quad (2)$$

where  $\sigma_0$  is a pre-exponential factor,  $E_a$  the activation energy,  $k$  the Boltzmann constant and  $T$  the temperature. From the exponential fit, a value for the activation energy of 0.79 was obtained.

In the case of 200nm SA thin films, a very different trend was observed. At room temperature the current dependence on the electric field is no longer linear, but it can be approximated by hyperbolic sinus (Fig. 5). This trend is characteristic of

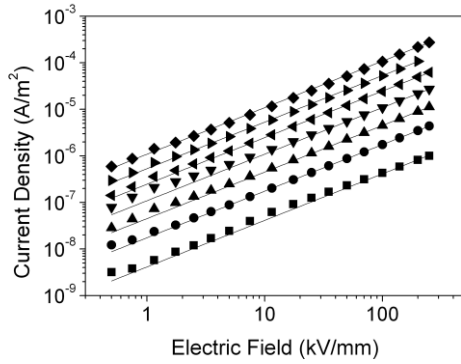


Fig. 3 Current density vs. electric field in 200nm GF PMMA thin films, at: ■, 25°C.; ●, 40°C.; ▲, 50°C.; ▼, 60°C.; ◀, 70°C.; ▶, 80°C.; ◆, 90°C. (calculated fits are represented by straight lines)

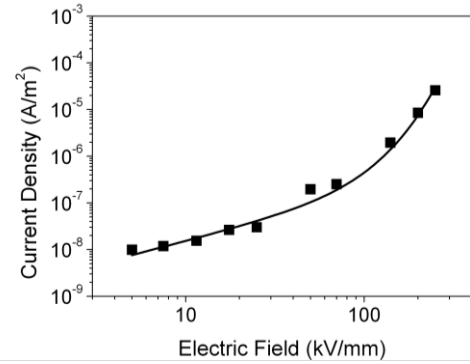


Fig. 5 Current density vs. electric field in 200nm SA PMMA thin films at T=25°C. (■, experimental points; —, calculated fit)

charge transport by “hopping” mechanism between shallow traps, which obeys the following expression:

$$J \propto \sinh\left(\frac{eFd}{2kT}\right) \quad (3)$$

where  $d$  is the distance between traps. By fitting the theoretical function to the experimental data, a value of  $d=1.4\text{nm}$  was extracted. At low fields (5-25kV/mm) the curve J-F can be approximated by a straight line, then the conduction can be considered as ohmic. Thereby, the conductivity can be estimated at  $1.09 \times 10^{-15}\text{S/m}$ . At higher temperatures, a steady current for fields higher than 17.5 kV/mm could not be obtained, and in some cases, even the breakdown took place.

Fig. 6 shows the Arrhenius diagram for 200nm SA thin films. The point corresponding to conductivity at 90°C lies out of the straight line fitting the other points. This can be explained by the closeness of the glass transition, despite in GF thin films no change in the trend was observed at such temperature. From the Arrhenius fit, the activation energy was found to be of 0.10eV. It is worth noting, for comparison purposes, that a trap depth of 0.15eV and an average distance between traps of 1.5nm have been estimated for polyethylene [8].

## 2) 50μm thick films

In the case of 50μm thick PMMA films, electrical fields as

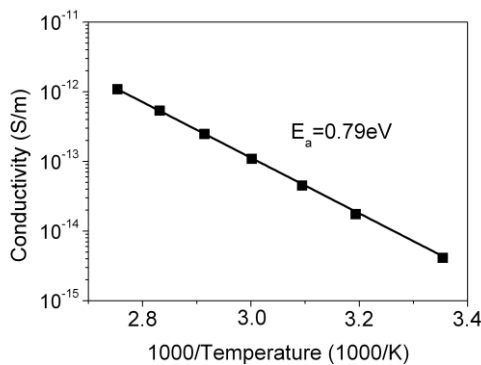


Fig. 4 Conductivity vs. reciprocal of temperature (Arrhenius diagram) in 200nm GF PMMA thin films. The calculated activation energy is displayed in the figure. (■, experimental points; —, calculated fit)

high as those used for thin films could not be applied. At low temperatures, the current needed too much time to stabilize and the discharge current was of the same order of magnitude as the charge current. So, the stationary conduction current could not be accurately obtained. However, by taking the polarization current along with the depolarization one, and assuming that the measurements are within the ohmic regime, the conductivity could be properly calculated [9]. The hypothesis of considering the electrical conduction as ohmic was verified by performing I(V) characteristics at temperatures over 50°C (Fig. 7). The calculated conductivity values increases from  $3.53 \times 10^{-17}\text{S/m}$  at 25°C, up to  $1.08 \times 10^{-14}\text{S/m}$  at 90°C. The estimated activation energy is 0.79eV (Fig. 8).

## IV. DISCUSSION

A summary of conduction mechanisms and extracted parameters is shown in Table I. 50μm GF thick films and 200nm GF thin films present the same conduction mechanism and similar activation energies. It consists in a charge transport by extended states thermally assisted by the detrapping of charge carriers at deep localized states (around 0.80eV of depth).

On the other hand, 200nm SA thin films show conduction by hopping mechanism between shallow localized states. Knowing that band structure and localized states are determined by chemical structure and polymer morphology,

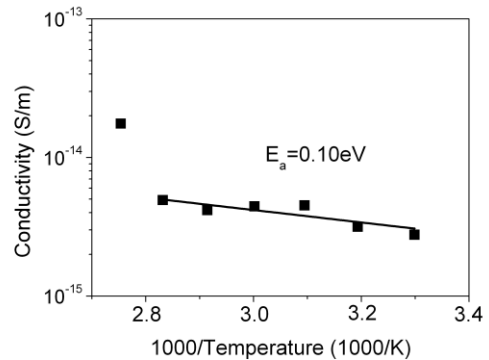


Fig. 6 Conduction vs. reciprocal of temperature (Arrhenius diagram) in 200nm SA PMMA thin films, for an electric field of 15kV/mm. The calculated activation energy is displayed in the figure. (■, experimental points; —, calculated fit)

TABLE I. SUMMARY RESULTS

Sample	Conductivity at Room Temperature (S/m)	Activation Energy (eV)	Electrical Conduction
GF 50 $\mu\text{m}$	$3.53 \times 10^{-17}$	0.79	Ohmic
GF 200 nm	$4.13 \times 10^{-15}$	0.79	Ohmic
SA 200 nm	$1.09 \times 10^{-15}$ (low fields)	0.10	Hopping

these differences between GF and SA thin films are consistent with the presence of a little amount of elastomer in GF PMMA (according to the supplier), whereas SA PMMA powder does not include any kind of additive. Furthermore, ohmic conductivity is found to be higher for thin films compared to thick films. We assume an effect of PMMA thickness on its conduction properties. As film thickness becomes closer to the polymer chain length, the possibility for charge carriers to cross the structure without changing the polymer chain increases. Also, the existence of large defects, like voids, becomes less probable. Such physical defects can hinder the charge carriers motion. Thus, the effective mobility should increase if the large defects amount is reduced. A similar reasoning could be applied to the dielectric strength. Since breakdown can be originated by defects like protrusions or voids [10], the breakdown strength would raise when the physical dimensions of the sample are lowered to the nanometric scale. Even so, a dielectric strength increase with a thickness decrease could be also explained by the theory of thermal breakdown caused by Joule heating [2].

However, charge retention measurements show that nanometric thin PMMA films present better charge retention capabilities than micrometric ones. This seems to be in contradiction with the fact that ohmic conductivity is apparently higher in the former. Nonetheless, conductivity has been determined from the current flowing through metallic coated films, while an electric field was applied. On the other hand, PMMA films analyzed by KFM were previously charged by an AFM tip, without any conductive coating on film surface. Thus, injected charges could be dissipated by surface conduction along with bulk charge transport. In addition, the traps responsible for the long-run charge retention are not necessary involved in the dominant charge transport process. For instance, while shallow traps can enhance the charge transport, the deep localized states

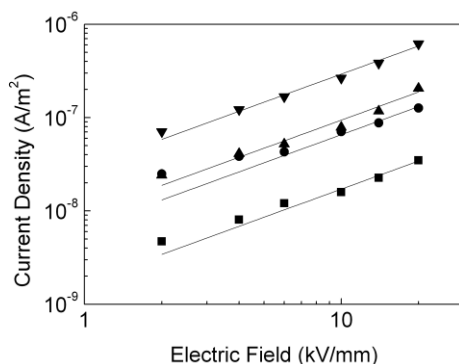


Fig. 7 Current density vs. electric field in 50 $\mu\text{m}$  GF thick PMMA films, at:  $\blacksquare$ , 60 $^{\circ}\text{C}$ .;  $\bullet$ , 70 $^{\circ}\text{C}$ .;  $\blacktriangle$ , 80 $^{\circ}\text{C}$ .;  $\blacktriangledown$ , 90 $^{\circ}\text{C}$ . (calculated fits are represented by straight lines)

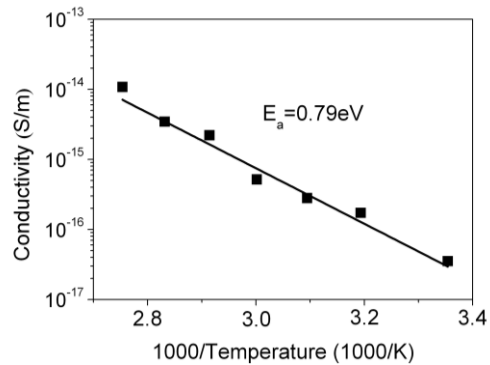


Fig.8 Conduction vs. reciprocal of temperature (Arrhenius diagram) in 50 $\mu\text{m}$  GF thick films, for an electric field of 20kV/mm. The calculated activation energy is displayed in the figure.

originate the steady trapped charge. In this sense, spin coating process, used for preparation of both GF and SA thin films, could lead to the incorporation of impurities that would act as deep traps. Further work on charge trapping, detrapping and recombination in PMMA films charged by AFM is needed to clear up the mechanisms involved in such processes.

#### ACKNOWLEDGMENT

This work was supported by the French National Agency (ANR) in the frame of its program 'Emergence' (Elec-NanoPrint project no ANR-2011-EMMA-015-01).

#### REFERENCES

- [1] J.H. Park, D.K. Hwang, J. Lee, S.I. and E. Kim, "Studies on poly(methyl methacrylate) dielectric layer for field effect transistor: Influence of polymer tacticity", *Thin Solid Films*, Vol. 515, pp. 4041-4044, 2007.
- [2] K. Miyairi and E. Itoh, "AC electrical breakdown and conduction in PMMA thin films and the influence of  $\text{LiClO}_4$  as an ionic impurity", 2004 Int. Conf. on Solid Dielectrics, Toulouse, France, 2004.
- [3] E. Palleau, N. M. Sangeetha, G. Viau, J. D. Marty and L. Ressler, "Coulomb Force Directed Single and Binary Assembly of Nanoparticles from Aqueous Dispersions by AFM Nanoxerography", *ACS Nano* Vol. 5, pp. 4228-4235, 2011.
- [4] A.N. Shipway, E. Katz and I. Willner, "Nanoparticle arrays on surfaces for electronic, optical, and sensor applications", *Chem. Phys. Chem.*, Vol. 1, pp. 18-52, 2000.
- [5] H.O. Jacobs and G.M. Whitesides, "Submicrometer patterning of charge in thin-film electrets", *Science*, Vol. 291, pp. 1763-1766, 2001.
- [6] L. Ressler, E. Palleau and S. Behar, "Electrical nano-imprint lithography", *Nanotechnology*, Vol.23, pp. 255302-255305, 2012.
- [7] L. Hartmann, W. Gorbatschow, J. Hauwede, and F. Kremer, "Molecular dynamics in thin films of isotactic poly(methyl methacrylate)", *Eur. Phys. J. E.*, vol. 8, pp. 145-154, 2002.
- [8] M. Meunier and N. Quirke, "Molecular modeling of electron trapping in polymer insulators", *J. Chem. Phys.*, vol. 113, pp. 369-376, 2000.
- [9] J. A. Diego, J. Belana, J. Orrit, J.C. Cañadas, M. Mudarra, F. Frutos and M. Acedo, "Annealing effect on the conductivity of XLPE insulation in power cable", *IEEE Trans. Dielectr. Electr. Insul.*, vol. 18, pp. 1554-1561, 2011.
- [10] J.C. Fothergill, G.C. Montanari, G.C. Stevens, C. Laurent, G. Teyssedre, L.A. Dissado, U.H. Nilsson and G. Platbrood, "Electrical, microstructural, physical and chemical characterization of HV XLPE cable peelings for an electrical aging diagnostic data base", *IEEE Trans. Dielectr. Electr. Insul.*, vol. 10, pp. 514-527, 2003.